AMERICAN METEOROLOGICAL SOCIETY

*Journal of Hydrometeorology*

# EARLY ONLINE RELEASE

This is a preliminary PDF of the author-produced manuscript that has been peer-reviewed and accepted for publication. Since it is being posted so soon after acceptance, it has not yet been copyedited, formatted, or processed by AMS Publications. This preliminary version of the manuscript may be downloaded, distributed, and cited, but please be aware that there will be visual differences and possibly some content differences between this version and the final published version.

The DOI for this manuscript is doi: 10.1175/JHM-D-14-0044.1

The final published version of this manuscript will replace the preliminary version at the above DOI once it is available.

If you would like to cite this EOR in a separate work, please use the following full citation:

Chen, X., M. Kumar, and B. McGlynn, 2014: Variations in streamflow response to large hurricane-season storms in a southeastern US watershed. J. Hydrometeor. doi:10.1175/JHM-D-14-0044.1, in press.

© 2014 American Meteorological Society

Manuscript (non-LaTeX)
Click here to download Manuscript (non-LaTeX): Manuscript.docx

AMERICAN METEOROLOGICAL SOCIETY 1919

# Variations in Streamflow Response to Large Hurricane-Season Storms in a Southeastern US Watershed

**Xing Chen, Mukesh Kumar AND Brian L. McGlynn**

*Nicholas School of the Environment, Duke University, Durham, North Carolina, USA*

PRELIMINARY ACCEPTED VERSION

**Corresponding author and address: Mukesh Kumar, Nicholas School of the Environment, Duke University, Durham, North Carolina, USA**

**Email: mukesh.kumar@duke.edu**

**Abstract**

Floods caused by hurricane storms are responsible for tremendous economic and property losses in the U.S. In order to minimize flood damages associated with large hurricane season storms, it is important to be able to predict streamflow amount in response to storms for a range of hydroclimatological conditions. However, this is challenging considering that streamflow response exhibits appreciable variability even for hurricane-season storms that deliver similar precipitation amounts. As such, better estimates of event responses require refined understanding of the causes of flood response variability. Here we use a physics-based, distributed hydrologic model and supporting hydrologic data sets to identify and evaluate dominant hydrologic controls on streamflow amount variability. Our analysis indicates that variability in flood response in the Lake Michie watershed is primarily driven by antecedent soil moisture conditions near the land surface and evapotranspiration during post-event streamflow recession periods, which in turn is a function of precipitation history and prevailing vegetation and meteorological conditions. Presented results and ensuing analyses could help prioritize measurements during observation campaigns and could aid in risk management by providing look-up diagrams to quickly evaluate flood responses given prior information about hurricane storm size.

## 1 Introduction

Hurricanes and tropical storms are major geophysical disaster-causing agents, which account for billions of dollars in annual property damages (Changnon 2009; Dale et al. 2001; Emanuel et al. 2008; Emanuel 1987; Saunders et al. 2000). In the United States alone, average annual losses caused by these storms exceeded $2.6 billion/year for the period 1949 to 2006 (Changnon 2009; Changnon and Changnon 1992). The majority of these storms originate in the Atlantic Ocean

between June and November (Changnon 2009) and cause extensive losses in the southeastern states of Louisiana, Florida, Georgia, South Carolina, and North Carolina. In North Carolina, where approximately 350 hurricanes have hit since 1667 (NOAA 2014; SCO 2014; USWB 1963; USWB et al. 1967), these storms have caused hundreds of fatalities and billions of dollars in property damages (Blake et al. 2007; NOAA 2013a, b). A large percentage of these losses have been due to flooding from intense storms (Ashley and Ashley 2008; NOAA 1996). To the dismay of water resource and risk managers, risks associated with remnant hurricanes and tropical storms are expected to increase in the future, as global warming is predicted to result in increased intensity of tropical disturbances (Easterling et al. 2000; Elsner 2007; Goldenberg et al. 2001; Knutson and Tuleya 2004; Landsea 2007; Mann and Emanuel 2006; Pielke et al. 2005; Salinger 2005; Webster et al. 2005).

Flooding related damages due to hurricane or other tropical disturbance storms can be considerably reduced if accurate prediction of streamflow response to these storms can be made. Prediction of flood responses to precipitation is non-trivial because they reflect more than just rain event size. For example, streamflow data from the Lake Michie watershed in North Carolina (Fig. 1 and Table 1) shows that streamflow response to large, similar magnitude (in terms of precipitation amount) hurricane-season storms can be significantly different. Note that hurricane-season storms in this paper indicate storms that have hurricane or other tropical-disturbance origins and happen between June and November. Events are defined to span from start of precipitation to the time after which there is no rainfall for at least six hours. The term event size and storm size have been used interchangeably throughout the paper, and refer to the amount of precipitation delivered during the storm event. Enormous variability in streamflow response is highlighted by dots falling within the vertical shaded bar in Fig. 1, where storms of size of

66 approximately 0.07 m are observed to generate streamflow with magnitudes varying by as much
67 as 250% around the mean. Additional details of these events are in rows 2, 5, 13 and 19 in Table
68 1 (identified by *). The flow magnitude in response to an event (in Fig. 1) is defined as the total
69 flow amount from the beginning of an event to the time when the recession limb flattens after the
70 end of that single storm. The observed variability of flood response suggests that, in addition to
71 storm event size, other transient controls such as evolving land surface characteristics and
72 hydrologic state may have significant influence on flow responses to storm events. While
73 previous studies have investigated contributing factors to streamflow generation during and
74 immediately after isolated hurricane storms (Castillo et al. 2003; Elsenbeer et al. 1995;
75 Sturdevant-Rees et al. 2001; Tramblay et al. 2010; Wood 1976), their influence on the variability
76 of flood response from one large hurricane-season storm to the other, both intra-annually and
77 inter-annually, has gone largely un-reported. This gap in knowledge is partially attributable to
78 the challenge associated with measurement of multiple hydrologic states over long periods of
79 time. Because hurricane and tropical storms are not a year-wise phenomenon, tracking the role
80 of controls on response variability would require multi-year data sets and detailed investigations.
81 This is expected to be a resource intensive task, as understanding of the influence of controls on
82 the variability of flood response would ideally require collocated observations within a
83 watershed that track partitioning across the hydrologic continuum, including surface flow,
84 evapotranspiration, vadose zone soil moisture, and groundwater response across multiple
85 hurricane-season storms.

86 The goal of this paper is to identify the causes of variability in flood response amount to
87 large hurricane-season storms. Variability in response from one event to another, even if the
88 events deliver similar precipitation amounts, is caused mainly by differences in transient controls

such as meteorological and antecedent hydrological conditions. Therefore, we specifically evaluate controls on streamflow variability from one storm event to next. The streamflow response discussed in this paper refers to the total discharge amount, rather than the peak discharge. Our case study utilizes publicly available observation data in synergy with a physically-based numerical watershed model and demonstrates the wide applicability of the approach in data poor regions.

## 2 Data and Methods

### *2.1 Study area and data sets*

We selected the Lake Michie watershed (LMW) in North Carolina as the study site to analyze the causes of variability in flood response to large hurricane-season storms. LMW is frequently struck by hurricane-season storms originating from the Atlantic Ocean. The watershed area is 432.8 sq. km and is part of the Neuse River Basin. Streamflow output from the watershed is delivered into the Lake Michie Reservoir, which serves as the primary water supply for city of Durham (population: 279,641 in 2012) since 1929 (Weaver 1994). Varied streamflow response to hurricane-season storms poses a significant challenge for effective reservoir management, water resource allocation, and risk assessment in the watershed, and thus underscores the need for better understanding of flood response.

The LMW is characterized by north-west to south-east oriented valleys, with elevation ranging from 87 to 270 m above sea level (Fig. 2d). Most of the watershed consists of gentle to moderately rolling hills with some steep, narrow valleys immediately upstream of the Lake Michie reservoir (Weaver 1994). Upland slopes range from 0 to 36 degrees. We used a 30 m

resolution digital elevation model grid data from USGS (USGS 2013a) for analyses. Climate in the watershed is characterized by long, hot, humid summers and short mild winters with transitional seasons (Kopec and Clay 1975). During year 1985 to 2012, average monthly temperature in the watershed ranged from 5 °C in January to 35 °C in July, while annual precipitation ranged from 802 to 1577 mm, with over half of the precipitation occurring during hurricane-season (June to November). Annual runoff ratios (evaluated as the ratio of annual streamflow discharge and precipitation amount) for this period ranged from 0.11 to 0.46. Here we used hourly climate data (including precipitation, temperature, relative humidity, wind velocity, solar radiation, and vapor pressure) from NLDAS-2 meteorological forcings dataset (Xia et al. 2012). Spatial resolution of all the aforementioned forcings data is 1/8° or approximately 9.5 km in LMW (Mitchell et al. 2004). The watershed consists of 15 land cover types based on National Land Cover Data (NLCD 2013). 56% of the watershed is covered by forest, while 34% of the total area is covered by shrubs. Forests in the watershed include deciduous, evergreen and mixed conifer trees, while shrubs include scrub, hay, grassland and crops. Percentage of developed area in the watershed is approximately 9% of the total area. SSURGO data (SSURGO 2013) indicates that the watershed consists of 33 soil composition types, with majority of the area covered with loamy soils.

### *2.2 Model description*

A physically-based, spatially distributed hydrologic model, PIHM (Penn State Integrated Hydrologic Model) (Kumar 2009; Kumar et al. 2009b; Qu and Duffy 2007), was used here to perform long-term integrated hydrologic simulations of streamflow and other coupled hydrologic states. PIHM employs a semi-discrete finite volume formulation to locally integrate partial differential equations of hydrologic processes to ordinary differential equations (ODEs) on each

unstructured mesh element (Fig. 2d). The system of ODEs defined on all mesh elements were assembled, and solved simultaneously with a stiff ODE solver using an implicit Newton-Krylov integrator. An adaptive time-stepping scheme is used for capturing model dynamics during period of rapid changes in states, triggered usually by precipitation pulse. The control volume elements used to discretize the domain include triangular and linear shaped units, which represent land surface elements and rivers, respectively. These elements are projected downwards to the bedrock (for land surface elements) or to the river bed (for river elements) to form prismatic or cuboidal elements respectively in 3D (Kumar 2009). The model was implemented on an unstructured mesh decomposition of the LMW (Fig. 2d), with 399 land elements (3D prismatic units) and 77 river segments (3D cuboidal units). Each land element was discretized into three layers: a top relatively thin unsaturated zone with thickness of 0.25 m, an intermediate unsaturated zone that extends from 0.25 m to groundwater level, and a groundwater layer. The two lower layers have variable dimensions, as they depend on the evolving groundwater table depth. Each river unit was vertically discretized into two layers, with flowing river on the top and a groundwater zone below it. Processes simulated in PIHM include snowmelt, evapotranspiration (Penman - Monteith equation), interception (Rutter model), overland flow (2D diffusion wave equations), unsaturated zone infiltration (1D approximation of Richards' equation), groundwater flow (3D Richards's equation), and streamflow (1D diffusive wave).

### *2.3 Model parameterization, calibration and validation*

A tightly-coupled GIS framework, PIHMgis (Bhatt et al. 2008, 2014), was used to parameterize the model domain using the aforementioned data sets (see section 2.1). This includes defining relations between hydrographic units and their physical properties. For more details about the

157 processes, parameters and topology of domain discretization, readers are referred to Kumar et al.
158 (2009a, 2010).

159 PIHM simulations were performed for twenty-eight years (1985 to 2012), for which
160 streamflow data is available for validation. Streamflow calibration was performed against
161 observed hourly streamflow data at USGS site id #2085500 (Fig. 2d), which lies 12.8 km above
162 the Lake Michie Reservoir. The calibration was performed for the year 2002, which received an
163 annual precipitation of 1142 mm, the same as the average precipitation for the entire simulation
164 period. The calibration process involved nudging hydrogeological parameters uniformly across
165 the model domain (Refsgaard and Storm 1996) to match the baseflow magnitude and
166 groundwater head distribution during dry periods, and the rate of hydrograph decay during
167 recession. Two calibration periods were chosen: (1) a summer period with no appreciable
168 recharge (late April to early June), and (2) a wet, cold period with substantial streamflow
169 response to precipitation and relatively low evapotranspiration (November to December). The
170 calibration process involved first initializing the PIHM model with water table at the land
171 surface, and then letting the model relax with no precipitation input until streamflow approaches
172 zero. The simulated relaxation hydrograph was compared with observed streamflow during the
173 first calibration period (identified above). Streamflow during this period was mostly dominated
174 by baseflow, which in turn was controlled by subsurface properties of the model domain. The
175 goal of this initial model calibration step was to identify sets of hydrogeologic properties, such as
176 van-Genuchten coefficients, macro and matrix porosities, and hydraulic conductivities, which
177 would allow reasonable match between modeled and observed base flow and groundwater head
178 distributions. The second calibration step involved comparing the simulated relaxation rates with
179 the observed values. Streamflow calibration results and corresponding model efficiencies in the

180 calibration year are shown in Fig. 3a. The dynamics of streamflow variation between observed
181 and modeled results are in reasonable agreement, and are considered acceptable. Similar
182 modeled and observed runoff ratios of 0.219 and 0.214 respectively (Table 2) also indicate
183 reliable partitioning of the water budget. Furthermore, annual evapotranspiration (*et*) estimation
184 of 660 mm in this watershed is in good agreement with estimated results from a nearby heavily
185 vegetated site (areal distance of 26.5 km from Lake Michie Reservoir) in Duke Forest, where *et*
186 was reported to range from 580 to 740 mm annually (Stoy et al. 2006).

187 Results of streamflow validation for 1985 to 2012 (Fig. 3b) show a Nash-Sutcliffe
188 efficiency (NSE) of 0.68 and $R^2$ of 0.83 for daily data, 0.80 and 0.90 for monthly data, and 0.72
189 and 0.89 for yearly data. It is to be noted that the watershed does not have any operationally
190 active groundwater wells within it that can be used to validate the temporal dynamics of
191 groundwater. This level of data scarcity is neither surprising nor unusual, and is typical for
192 watersheds of this size. In fact, the density of USGS groundwater observation wells in the
193 contiguous US is less than 1 well per 6150 sq. km (USGS 2013b). However, single-instance
194 groundwater depth data does exist at 36 locations within the watershed. Modeled groundwater
195 elevation heads are compared to the observed data for respective dates to evaluate the ability of
196 model in capturing the spatial distribution of groundwater level (Jones et al. 2008). The results
197 show good agreement between simulated and observed groundwater elevation head with $R^2$ =
198 0.89 (Fig. 3c), indicating that the distribution of modeled total groundwater heads reasonably
199 matches the observed data. Notably, the target metrics of the calibration strategy -- the rate of
200 hydrograph decay during cold period, and the magnitude of baseflow and spatial distribution of
201 groundwater table depth during summer -- differ from the validation metrics such as the match
202 between simulated and observed streamflow time series and static groundwater table depths. The

goal was to avoid simply fitting parameters to match observed data, while attempting to best represent the underlying behavior and response dynamics of the watershed. Since no soil moisture monitoring stations exist within the watershed, soil moisture data from the nearest ECONET site (SCONC 2014) in Durham, which is 13 km south of the watershed, was used for validation. Because of the similarity in both timing and magnitude of the precipitation at the soil moisture site and that within the LMW, it is reasonable to expect that soil moisture dynamics at the ECONET site should show similar patterns to that in the LMW, especially at locations within the watershed that have the same land cover and soil type. It is to be noted the landscape slope was also very similar (~4.5°) at the two comparison sites. Modeled soil moisture deficit at these locations (with same land cover and soil type as at the soil moisture monitoring site) within the LMW watershed are compared to observed data at ECONET site for 2009 to 2010 (Fig. 3d). The soil moisture deficit is defined as the fraction of pore space in top 0.25 m of subsurface that needs to be filled by moisture before saturation occurs. Similar variations and ranges of moisture deficit between modeled and observed data suggest that the model was able to capture soil moisture dynamics to an acceptable degree. It is to be noted that soil moisture data after 2010 was not included in this analyses because of changes in instrument setup at the site and outstanding re-calibration needs.

Since the focus of this paper is on the variability of streamflow response to large hurricane-season storms, further confidence in the model result in this context was built by evaluating the ability of the model to simulate the order-sequence of streamflow responses corresponding to large hurricane-season storms. Rank correlation coefficient (*rccQ*) of modeled and observed streamflow amounts corresponding to the top 50 hurricane-season storms (in terms of size) for the period 1985 to 2012 was calculated. For each event, streamflow amount under the

hydrograph was calculated from the start of the event until the recession limb flattened. Flattening of the recession limb was identified by flow difference of less than 80 $m^3$ in an hour, which is approximately 1% of the average flow rate from the watershed during hurricane-season. Since some of these large events were immediately followed by other precipitation events at close time intervals, making it difficult to account for the streamflow response explicitly due to an event in consideration, *rccQ* was calculated only for events where streamflow contribution could be quantified without the convolved influence of following precipitation events. Rank correlation (*rccQ*) for these events was estimated to be equal to 0.81. This suggests that the PIHM simulations also reasonably captured the relative variability in streamflow response across multiple events.

The aforementioned validation results of streamflow, groundwater, soil moisture, and *et*, at scales ranging from events to seasons to decades, establishes sufficient confidence in the model performance for it to be used in evaluation of the role of controls on streamflow response variability to large hurricane-season storms.

### *2.4 Understanding the role of controls on variable flood response from model results*

Variability in flood response to hurricane-season storms can be either due to differences in meteorological forcings or changes in watershed-response dynamics across different events. For events that deliver similar precipitation amounts, variations in hydrologic response (streamflow amount) can be caused by differences in transient controls such as antecedent hydrologic states and/or evolving watershed properties such as seasonal variation in ecohydrologic functions (e.g. transpiration and interception loss) of vegetation and meteorological forcings. In order to identify the controls on variability in flood response arising from large hurricane-season storms, we first quantified the streamflow contribution due to an event, and then compared the hydrologic

process contributions between events of similar sizes but considerably different responses. The first step was not trivial, considering that an observed streamflow discharge time series was often also comprised of flow due to subsequent events that happened well before the influence of previous events on the streamflow hydrograph had subsided. To isolate the flow response generated only due to a particular precipitation event, we conducted event-scale PIHM simulations in addition to the long-term PIHM simulation (which was presented in section 2.3). The event streamflow simulations were run from the start of the precipitation event to the time by which generated stream flow recession limb flattened. Event simulations used observed meteorological forcings as inputs, while antecedent hydrologic conditions were set based on the results of the long term simulation. Fig. 4 shows simulated discharge obtained from the event simulation (*eventQ*) and discharge per unit event size (*eventQ/p*), for the largest 50 hurricane-season storms (in terms of delivered precipitation amount) during the 28-year simulation period. Large spread in flow response, even for events of similar sizes, is highlighted through two event-pairs of magnitudes 0.067 m (events A and B), and 0.102 m (C and D) respectively (Table 1 and Fig. 4a). For the 0.067 and 0.102 m storm sizes, *eventQ/p* varies from 0.13 to 0.66 m/m and 0.18 to 0.35 m/m respectively, suggesting that runoff ratios can vary by more than 100 percent in response to events of approximately the same size.

In order to understand the causes of differential streamflow response to similar sized hurricane-season storms, hydrologic stores that vary markedly across the events were identified. For this, we considered the two event-pairs with similar event size, identified earlier in Table 1 and Fig. 4. For each pair, the source of difference in streamflow response was first determined by comparing water partitions between different hydrologic stores (Table 3). It is to be noted that water partitions in all hydrologic stores were estimated from the start of the precipitation event to

the time by which generated stream flow recession limb flattened. Since the summation of evapotranspirative loss (*et*), net change in storage (*delS*) and streamflow depth (*eventQ*) equals the precipitation magnitude (*p*), i.e., $p=et+delS+eventQ$; for events of similar sizes, difference in *eventQ* has to be due to differences in *et* and *delS* terms. For events A and B, *eventQ* differs by 0.018m. This difference is primarily attributable to the variation in net storage between events (0.015m) as difference in *et* between the two events ($\Delta et$) is only 0.002. Larger $\Delta delS$ could be due to differences in antecedent conditions during the events. In contrast, a difference of 0.035m in *eventQ* between events C and D is dominantly due to the difference in *et* (0.024m). This could be due to differences in meteorological conditions, or transpiration and interception capability of vegetation between the two events. To identify the role of hydrologic controls on changes in hydrologic stores and hence the flood response, additional event simulations were conducted by removing the influence of controls one at a time. The role of these controls on a larger set of hurricane-season storms was subsequently tested by evaluating correlation between streamflow amount (*eventQ*) and effective precipitation size (*effP*) of hurricane-season events. It is to be noted that *effP* for an event was evaluated by calculating the difference between precipitation event size and the "negative water store" term, which includes evapotranspirative loss (*et*) and the moisture storage deficit (*d*) that needs to be filled before streamflow is generated. For example, *effP* for an event, during which the soil is completely saturated, is equal to the event precipitation magnitude *p* minus *et*. If the ground is unsaturated and streamflow due to a precipitation event is generated only after the top soil layer gets saturated (after the moisture deficit has been filled), *effP* is evaluated as $p-(et+d)$. Henceforth, correlation coefficient between *eventQ* and *effP* was compared to correlations between *eventQ* and *p*. A higher correlation between *effP* and *eventQ* would indicate that hydrologic stores used in evaluation of *effP* play an

295 important role in determining streamflow response. In contrast, a lower or negligible change in
296 correlation coefficient with respect to correlation between *p* and *eventQ* would suggest that
297 streamflow response is not sensitive enough to the concerned hydrologic store (/s) that is (/are)
298 used in evaluation of *effP*.

299

300 **3 Results and Discussion**

301 *3.1 Role of watershed antecedent hydrologic conditions on variable streamflow response*

302 Comparison of water budget partitions for events A and B (see Table 3) shows that *delS* during
303 event B (0.069 m) was larger than during event A (0.054 m), thus indicating that difference in
304 net storage (Δ*delS*) played an important role in disparity in streamflow response between the two
305 events. It is to be noted that *delS* for an event is defined as the difference in total subsurface soil
306 moisture content (both in unsaturated and saturated zone) between start and end of an event
307 simulation. Marked difference in *delS* (equal to 83% of the difference in streamflow response
308 amount) between the two events could be attributed to larger moisture deficit in both the near-
309 surface soil layer and the groundwater table for event B. To isolate the role of antecedent
310 hydrologic conditions (and hence moisture deficit) on variability in flood response, an additional
311 event simulation, A1, was conducted. The modeling configuration (watershed properties and
312 meteorological conditions) of event simulation A1 was set exactly the same as that of event A,
313 however, the antecedent conditions were set identical to event B. Results from event simulation
314 A1 suggest that the flood response amount of event A would be much less, and also very similar
315 to that of event B, if the antecedent conditions of B were used. This confirms that antecedent
316 conditions plays a dominant role in varied response of events A and B, and could be an important
317 factor in determining wide-range of streamflow responses to hurricane-season storms in general.

It should be noted, however, that event simulation A1 does not fully identify if the moisture deficit near the land surface (say in top 25 cm) is the major contributor to differential response, or if differences in groundwater table depths are also important. To explore this further, two additional experiments (A2 and A3) were conducted. Simulation configuration of A2 was set exactly the same as A, but the groundwater initial condition was set identical to that of event B. Simulated flood response amount for event A2, which only marginally differed from that of event A, indicated that groundwater depth did not play a substantial role in determining varied responses between events A and B. In contrast, event simulation A3, which has the same configuration as A but with surface soil (top 25 cm) moisture identical to B, showed a flood response amount that was more akin to event B, thus confirming that surface soil moisture was the primary driver for the disparity in responses between event A and B. The role of antecedent moisture conditions in varied streamflow responses was also evident for event pairs (20 and 27) and (21 and 39) in Table 1, where streamflow response was also significantly larger when antecedent soil moisture was higher. These results highlight that differences in individual hydrologic stores (unsaturated zone or ground water) can play as significant a role as differences in total storage in determining varied streamflow response to hurricane-season storms.

We examined variations in surface flow depth, near the land surface saturation (top 25 cm) and groundwater depth during events A and B to further understand how soil moisture deficit near the land surface influences variability in response even while groundwater initial conditions has negligible impact on it (Fig. 5). For certain periods during both the events, simulation results suggested that the top 25 cm was saturated in most of the watershed. However, the groundwater table was never that shallow anywhere in the watershed during the time of saturation (Fig. 5a-b). This indicates that overland flow generated during saturation (shown in

Fig. 5c-d) was primarily because of an infiltration excess process resulting from saturation in the near surface soil. It should be noted that the absence of transient groundwater observation data within the watershed makes it difficult to absolutely confirm that groundwater table does not reach the land surface during the period when surface soil experiences saturation, as was simulated by the model. However, observed groundwater level time series from a neighboring watershed (NC-DWR Caldwell site # F43X1, the site is 19.3 km from LMW outlet) (NCDWR 2014), confirmed that groundwater table never reached the land surface even in the valley floor during the entire observation period (1985 to 2012). Additionally, soil saturation data at ECONET site (Fig. 3d), which incidentally also exists outside the LMW (see section 2.3) confirmed that the near surface soil moisture did reach saturation during hurricane-season storms, as was also simulated by the model. Since infiltration excess due to near surface saturation was the cause of overland flow generation during the two events, lower antecedent soil saturation (*SS*) for event D (Table 3 and Fig. 5a) meant that larger soil moisture deficit had to be satisfied before overland flow can be generated. Hence, antecedent soil saturation conditions near the land surface can play a crucial role in determining surface flow response. Since overland flow contribution to streamflow during events A and B was as large as 97% and 98% respectively, antecedent soil moisture conditions near the land surface ended up being the primary determinant of the varied response in events A and B.

To evaluate the role of near land surface moisture deficits on variable responses due to large hurricane-season storms in general, the correlation coefficient between streamflow amount (*eventQ*) and effective precipitation size (*effP*), evaluated here as (*p*-*d*) where *d* is the moisture deficit in the top 25 cm, was compared to the correlation between *eventQ* and *p* for all top 50 hurricane-season events. Improved $R^2$ of 0.77 for *eventQ* vs. *effP* (Fig. 6b) with respect to *eventQ*

364 vs. *p* (Fig. 6a) indicate that soil moisture deficit is indeed an important determinant in variability
365 of streamflow response, and hence also on its predictability. Notably, $R^2$ between *eventQ* vs. *effP*
366 for the case when *effP* is evaluated as (*p*-*d*), where *d* is the moisture deficit defined by
367 groundwater table depth, reduced to 0.44, thus re-confirming that groundwater level did not play
368 a substantial role in variability of streamflow response and hence in its predictability.

369 It should be noted that the differences in antecedent soil saturation conditions, which
370 influenced the streamflow response, may themselves be controlled by previous precipitation. To
371 explore this further, coefficient of determination ($R^2$) between antecedent soil moisture and total
372 precipitation amount in the previous N days (where N is a positive integer) were evaluated.
373 Results reveal that precipitation in the previous 1, 4, 8, 15 and 30 days explained 6.4, 22.4, 24.8,
374 22.7 and 16.6% of the variance in antecedent soil moisture. Sizable $R^2$ values indicate that
375 precipitation history did influence the antecedent soil moisture, and hence hydrologic response to
376 large storms. Furthermore, a maximum $R^2$ for N = 8 days suggests that the soil-moisture memory
377 of the watershed was approximately one week.

378 *3.2 Role of evapotranspiration (et) on variable streamflow response*

379 Comparison of water budget partition in events C and D (see Table 3) shows that
380 evapotranspiration loss plays an important role in the disparity in streamflow response. *et* during
381 event D (0.031 m) was markedly larger than during event C (0.007 m). It is to be noted again that
382 *et* is the total evapotranspiration during the streamflow event, which spans from the start of the
383 storm to the time by which generated stream flow recession limb has flattened. Notably,
384 evapotranspirative losses during the storm periods are relatively small (0.002m and 0.006m for
385 event C and D, respectively), and hence marked difference in *et* between the two events is
386 because of losses that happen after the storm, a major component of which is due to transpiration

of infiltrated water in the root zone. The difference in *et* rate during post-storm periods is attributable to favorable meteorological (higher temperature and radiation conditions) and ecological (higher leaf area index) conditions in August relative to November (when event C happened). It is to be noted that antecedent conditions for events C and D were also different, and could also play a role in differential responses by influencing both *et* and *delS*. To isolate the influence of meteorological conditions and vegetation states on *et*, a new event simulation, C1, was conducted. Event C1 replicates event C, but with an assumption that it happens in August (at the same time as event D). This means that meteorological and vegetation conditions during C1 were the same as that during event D. Expectedly, *et* for event C1 was much larger than in event C, thus reinforcing the fact that difference in *et* between events C and D was largely due to their timing and differences in potential evapotranspiration. Notably, a relatively large evapotranspiration loss in C1 in relation to event D, does not translate to a very small flood response, as was the case in event D. This suggests that antecedent conditions could also be playing a role in differential response. To evaluate the role of antecedent conditions, event simulation C2 was conducted with exactly the same modeling configuration as event C, but with antecedent conditions that were set identical to event D. Results suggest that while *eventQ* in this case is relatively smaller than event C, it is still markedly different than *eventQ* in event D. The combined effect of differences in antecedent conditions and *et* was evaluated by event simulation C3, which has the same timing and antecedent conditions as event D. Simulated flood response amount for event C3, now only marginally differed from that of event D. This indicates that both *et* and moisture deficit contributed to varied responses between events C and D. The combined effect of *et* and moisture deficit is evident in the event pair 15 and 26 (see Table 1), for which the streamflow responses are almost the same even though event 26 had a much higher antecedent

410 soil moisture. This is because of much larger *et* during the post-event streamflow recession
411 period of event 26, as it occurs in July when potential evapotranspitation rates are relatively
412 larger.

413 To evaluate the role of differences in *et* on variable flood responses due to large
414 hurricane-season storms, correlation coefficients between *eventQ* and *effP* were evaluated for the
415 largest 50 hurricane-season storms during the simulation period. Here *effP* is calculated as (*p*-*et*).
416 Improved $R^2$ of 0.73 (Fig. 6c) with respect to *eventQ* vs. *p* (Fig. 6a) indicates that *et* was indeed
417 an important determinant in variability of streamflow response, and hence also on its
418 predictability. It is to be noted that variations in *et* are often rooted in differences in timing of
419 respective events, as timing determines both the vegetation states and meteorological conditions
420 that are conducive to *et*. This suggests that variability in flood response due to hurricane-season
421 storms can sometimes be simply related to timing of the event within a year, with smaller
422 response expected in summer (June to August) when *et* is as large as 40% of event precipitation.

423 The integrated role of antecedent conditions and *et* on the variability of flood response due
424 to largest 50 hurricane-season storms was further evaluated by recalculating the correlation
425 between *eventQ* and *effP*, where *effP* is calculated as (*p*-*et*-*d*). Improved $R^2$ of 0.83 (Fig. 6d)
426 confirms the potential role of both *et* and antecedent near-surface soil moisture conditions on the
427 variability of streamflow response amount. Further analyses suggest that the average "missing"
428 percentage of precipitation (quantified as $100\times(1-eventQ/p)$) for the largest 50 hurricane-season
429 storms was as large as 74% of the precipitation amount, of which approximately 52 and 22%
430 were lost to soil moisture deficit and evapotranspiration respectively. The results indicate that
431 antecedent soil moisture was the dominant control on streamflow response. Event based analyses
432 showed that antecedent soil moisture was the primary control on streamflow response in 28 out

433 of 50 top hurricane-season storms, while evapotranspirative losses were dominant in 22 storms.
434 Relative dominance of the two controls on streamflow response showed a seasonal trend, with
435 antecedent soil moisture being the dominant control for 73.5% of large hurricane-season storms
436 during August to November. In contrast, evapotranspiration was the main determinant in 87.5%
437 of the large hurricane-season storms between June and July.

438

439 **4 Conclusions and Synthesis**

440 This paper evaluates the extent of variability in streamflow response due to large hurricane-
441 season storms, and examines the role of transient hydrologic controls on the said variability.
442 Analyses were conducted based on model simulation results obtained from a physically-based
443 integrated hydrologic model, PIHM, which was validated for multiple states within the Lake
444 Michie watershed including streamflow hydrograph, runoff ratio, groundwater table elevation,
445 soil moisture and ranges of evapotranspiration. To confirm the applicability of the model for
446 analyses of variability in streamflow response, ranks of predicted streamflow responses were
447 validated. The validated model was then used to perform nested control event simulations to
448 quantify the variability in streamflow response, and to identify and isolate the role of hydrologic
449 controls on different water stores during storm events. Analyses suggest that hurricane-season
450 storms of similar size could generate a considerable range of streamflow responses (more than
451 100% difference), thus highlighting that it is not reliable to use storm size alone to predict the
452 streamflow response and the consequent flood. Event simulations suggest that the dominant
453 controls on the variability of streamflow amount were soil saturation near the ground surface,
454 and evapotranspirative losses, which are in turn influenced by meteorological conditions and
455 vegetation states. Generally, higher antecedent topsoil saturation would lead to generation of

larger streamflow in response to events of similar sizes. Also, since meteorological conditions and eco-hydrologic functions of vegetation follow a seasonal variation, streamflow response shows a strong dependence on timing of the event within a year. For example, streamflow amount, in response to events of similar sizes, is much less for events that happen in July with respect to the ones that happen in November. Notably, groundwater contribution on streamflow amount under hurricane-season storms is negligible. The role of identified controls on varied streamflow responses for a wider set of hurricane-season storms was evaluated by calculating the predictability of streamflow response size after accounting for the role of controls. Increased correlation between streamflow response size and effective storm size, which accounts for the role of controls, compared to that between streamflow amount and precipitation alone further reinforced the role of individual hydrologic controls. Between antecedent topsoil saturation and post-event evapotranspiration, the former was identified as the dominant control on streamflow response amount. However, evapotranspiration was still a primary determinant on streamflow response, especially during June and July.

Information regarding the dominant controls on variability of streamflow response can be used to help prioritize resources for field campaigns and observation systems. For example, distributed measurements of soil moisture, which plays a crucial role in determining flood response, can be used in assimilation of antecedent soil moisture states, regionalization of relevant sensitive model parameters and validation of model results, thus leading to an improved predictability and reduced uncertainty in estimation of flood response to large hurricane-season storms. In contrast, a much refined groundwater network, although important, might not sufficiently improve the prediction of flood response to hurricane-season storms. Knowledge of process controls and antecedent conditions can also be used to aid in risk management by

479 providing look-up diagrams to quickly evaluate flood responses, given prior information about
480 hurricane storm size. This may be realized through development of a streamflow response map
481 for a range of antecedent conditions, timings of hurricane storms, and event sizes in a watershed.
482 One simplistic, but representative example of a look-up diagram is shown in Fig. 7 which shows
483 streamflow response to three hurricane storms of varying sizes, happening at different times
484 (June, September and November), and during dry, intermediate and wet antecedent states. A
485 look-up diagram of this sort, with responses mapped at finer resolutions and for a wide range of
486 conditions, could be used by resource managers to easily estimate the flood response size due to
487 an impending hurricane storm. In addition, comparison of look-up diagrams or storm-response
488 maps among different watersheds can also provide information about which watershed is more
489 vulnerable to events of a particular size. It should be noted that the two dominant controls on the
490 variability in flood response documented here: antecedent soil moisture, and evolving vegetation
491 states and meteorological conditions, can be both estimated using remote sensing data. This
492 points to the potential for using satellite data to improve flood prediction due to hurricane-season
493 storms. It is to be noted that the dominant hydrologic controls identified in the LMW watershed
494 might not be applicable in all the south-eastern U.S. watersheds due to differences in
495 topographic, physiographic and other hydrogeologic properties such as soil drainage parameters
496 and vegetation types, all of which can influence infiltration and evapotranspiration rates. In
497 addition, while validation process took advantage of available hydrologic dataset within and
498 around the Lake Michie watershed, further confidence in the model performance and analyses
499 could be built by observing additional hydrologic variables for validation, such as transient
500 groundwater depth and evapotranspiration.
501

**Acknowledgements**

This study was supported by grants from the NSF-EAR1331846 Calhoun Critical Zone Observatory, Ecosystem and Water Working Group seed grant from the Nicholas Institute, and the Duke University start-up fund for new faculty. We would also like to thank all three anonymous reviewers for their constructive comments that greatly improved this manuscript.

507 **References**

508 Ashley, S. T., and W. S. Ashley, 2008: Flood Fatalities in the United States. *J. Appl. Meteoro.*
509 *Climatol.*, **47,** 805-818.

510 Bhatt, G., M. Kumar, and C. J. Duffy. Bridging gap between geohydrologic data and Integrated
511 Hydrologic Model: PIHMgis. *International Environmental Modelling and Software*
512 *Society (iEMSs)*, Barcelona, Catalonia (2008): 743-750.

513 Bhatt, G., M. Kumar, and C. J. Duffy, 2014, A tightly coupled GIS and distributed hydrologic
514 modeling framework, Environmental Modeling and Software (*Accepted*).

515 Blake, E. S., C. W. Landsea, and E. J. Gibney, 2007: *The deadliest, costliest, and most intense*
516 *United States tropical cyclones from 1851 to 2006 (and other frequently requested*
517 *hurricane facts).* NOAA/National Weather Service, National Centers for Environmental
518 Prediction, National Hurricane Center, 47 pp.

519 Castillo, V. M., A. Gomez-Plaza, and M. Martinez-Mena, 2003: The Role of Antecedent Soil
520 Water Content in The Runoff Response of Semiarid Catchments: A Simulation
521 Approach. *J. Hydrol.*, **284,** 114-130.

522 Changnon, S., 2009: Characteristics of Severe Atlantic Hurricanes in The United States: 1949-
523 2006. *Nat. Hazards*, **48,** 329-337.

524 Changnon, S., and J. Changnon, 1992: Temporal Fluctuations in Weather Disasters: 1950-1989.
525 *Climatic Change*, **22,** 191-208.

526 Dale, V. H., and Coauthors, 2001: Climate Change and Forest Disturbances: Climate change can
527 affect forests by altering the frequency, intensity, duration, and timing of fire, drought,

introduced species, insect and pathogen outbreaks, hurricanes, windstorms, ice storms, or landslides. *BioSci.*, **51,** 723-734.

SCONC, cited 2014: References. [Available online at http://hatteras.meas.ncsu.edu/cronos/?station=DURH&temporal=daily.]

Easterling, D. R., G. A. Meehl, C. Parmesan, S. A. Changnon, T. R. Karl, and L. O. Mearns, 2000: Climate Extremes: Observations, Modeling, and Impacts. *Sci.*, **289,** 2068-2074.

Elsenbeer, H., D. Lorieri, and M. Bonell, 1995: Mixing Model Approaches to Estimate Storm Flow Sources in an Overland Flow-Dominated Tropical Rain Forest Catchment. *Water Resour. Res.*, **31,** 2267-2278.

Elsner, J. B., 2007: Granger causality and Atlantic hurricanes. *Tellus A*, **59,** 476-485.

Emanuel, K., R. Sundararajan, and J. Williams, 2008: Hurricanes and Global Warming: Results from Downscaling IPCC AR4 Simulations. *Bull. Amer. Meteoro. Soc.*, **89,** 347-367.

Emanuel, K. A., 1987: The dependence of hurricane intensity on climate. *Nat.*, **326,** 3.

Goldenberg, S. B., C. W. Landsea, A. M. Mestas-Nuñez, and W. M. Gray, 2001: The Recent Increase in Atlantic Hurricane Activity: Causes and Implications. *Sci.*, **293,** 474-479.

Jones, J. P., E. A. Sudicky, and R. G. McLaren, 2008: Application of a fully-integrated surface-subsurface flow model at the watershed-scale: A case study. *Water Resour. Res.*, **44,** W03407.

Knutson, T. R., and R. E. Tuleya, 2004: Impact of CO2-Induced Warming on Simulated Hurricane Intensity and Precipitation: Sensitivity to the Choice of Climate Model and Convective Parameterization. *J. Climate*, **17,** 3477-3489,3491-3495.

549 Kopec, R. J., and J. W. Clay, Eds., 1975: *Climate and air quality, in North Carolina arlas:*
550 *Portrait of a changing southern state, 1975*. 20 pp.

551 Kumar, M., 2009: Toward a Hydrologic Modeling System. Ph.D., The Pennsylvania State
552 University, 274 pp.

553 Kumar, M., G. Bhatt, and C. J. Duffy, 2009a: An efficient domain decomposition framework for
554 accurate representation of geodata in distributed hydrologic models. *Int. J Geogr. Inf.*
555 *Sci.*, **23,** 1569-1596.

556 Kumar, M., C. J. Duffy, and K. M. Salvage, 2009b: A second-order accurate, finite volume-
557 based, integrated hydrologic modeling (FIHM) framework for simulation of surface and
558 subsurface flow. *Vadose Zone J.*, **8,** 873-890.

559 Kumar, M., G. Bhatt, and C. J. Duffy, 2010: An object-oriented shared data model for GIS and
560 distributed hydrologic models. *Int. J. Geogr. Inf. Sci.*, **24,** 1061-1079.

561 Landsea, C., 2007: Counting Atlantic tropical cyclones back to 1900. *Eos, Trans. Amer.*
562 *Geophys. Union*, **88,** 197-202.

563 Mann, M. E., and K. A. Emanuel, 2006: Atlantic hurricane trends linked to climate change. *Eos,*
564 *Trans. Amer. Geophys. Union*, **87,** 233-241.

565 Mitchell, K. E., and Coauthors, 2004: The multi-institution North American Land Data
566 Assimilation System (NLDAS): Utilizing multiple GCIP products and partners in a
567 continental distributed hydrological modeling system. *J. Geophys. Res.*, **109,** D07S90,
568 doi:10.1029/2003JD003823.

569 National Land Cover Datasets, cited 2013: References. [Available online at
570 http://www.mrlc.gov/nlcd2006.php.]

571 NOAA National Climatic Data Center - Storm Events Database (North Carolina), cited 2014:
572 References. [Available online at
573 http://www.ncdc.noaa.gov/stormevents/listevents.jsp?beginDate_mm=01&beginDate_dd
574 =01&beginDate_yyyy=1996&endDate_mm=04&endDate_dd=30&endDate_yyyy=2013
575 &eventType=%28Z%29+Hurricane+%28Typhoon%29&county=ALL&zone=ALL&sub
576 mitbutton=Search&statefips=37%2CNORTH+CAROLINA.]

577 NOAA Preliminary Report Hurricane Fran 1996, cited 2013a: References. [Available online at
578 http://www.nhc.noaa.gov/1996fran.html.]

579 NOAA Historical Hurricane Tracks, cited 2013b: References. [Available online at
580 http://csc.noaa.gov/hurricanes/.]

581 North Carolina, Division of Water Resources, cited 2014: References. [Available online at
582 http://ncwater.org/Data_and_Modeling/Ground_Water_Databases/leveldetail.php?quado
583 =F**43X1.]

584 Pielke, R. A., C. Landsea, M. Mayfield, J. Laver, and R. Pasch, 2005: Hurricanes and Global
585 Warming. *Bull. Amer. Meteoro. Soc.*, **86,** 1571-1575.

586 Qu, Y., and C. J. Duffy, 2007: A semidiscrete finite volume formulation for multiprocess
587 watershed simulation. *Water Resour. Res.*, **43,** W08419.

588 Refsgaard, J. C., and B. Storm, 1996: Construction, Calibration And Validation of Hydrological
589 Models. *Distributed Hydrological Modelling*, M. Abbott, and J. Refsgaard, Eds., Springer
590 Netherlands, 41-54.

591 Salinger, M. J., 2005: Climate Variability and Change: Past, Present and Future – An Overview.
592 *Climatic Change*, **70,** 9-29.

593 Saunders, M. A., R. E. Chandler, C. J. Merchant, and F. P. Roberts, 2000: Atlantic hurricanes
594 and NW Pacific typhoons: ENSO spatial impacts on occurrence and landfall. *Geophys.*
595 *Res. Lett.*, **27,** 1147-1150.

596 SCO, cited 2014: References. [Available online at http://www.nc-
597 climate.ncsu.edu/climate/hurricanes/affecting.php?state=NC&buffer=150].

598 SSURGO, cited 2013: References. [Available online at
599 http://soils.usda.gov/survey/geography/statsgo/.]

600 Stoy, P. C., and Coauthors, 2006: Separating the effects of climate and vegetation on
601 evapotranspiration along a successional chronosequence in the southeastern US. *Global*
602 *Change Biol.*, **12,** 2115-2135.

603 Sturdevant-Rees, P., J. A. Smith, J. Morrison, and M. L. Baeck, 2001: Tropical storms and the
604 flood hydrology of the central Appalachians. *Water Resour. Res.*, **37,** 2143-2168.

605 Tramblay, Y., C. Bouvier, C. Martin, J.-F. Didon-Lescot, D. Todorovik, and J.-M. Domergue,
606 2010: Assessment of initial soil moisture conditions for event-based rainfall–runoff
607 modelling. *J. Hydrol.*, **387,** 176-187.

608 USGS Digital Elevation Map, cited 2013a: References. [Available online at
609 http://nationalmap.gov/viewer.html.]

610 USGS Groundwater site inventory of the nation, cited 2013b: References. [Available online at
611 http://waterdata.usgs.gov/nwis/inventory.]

612 USWB, 1963: *North Carolina hurricanes; a descriptive listing of tropical cyclones which have*
613 *affected the State.* For sale by the Superintendent of Documents, U.S. Govt. Print. Off.,
614 26 pp.

615 USWB, C. B. Carney, and A. V. Hardy, 1967: *North Carolina hurricanes; a listing and*
616 *description of tropical cyclones which have affected the State.* Rev. ed., 40 pp.

617 Weaver, J. C., 1994: Sediment Characteristic and Sedimentation Rates in Lake Michie, Durham
618 County, North Carolina, 1990-92, Water-Resourse Investigation Report 94-4123 Rep, 38
619 pp.

620 Webster, P. J., G. J. Holland, J. A. Curry, and H.-R. Chang, 2005: Changes in Tropical Cyclone
621 Number, Duration, and Intensity in a Warming Environment. *Sci.*, **309,** 1844-1846.

622 Wood, E. F., 1976: An analysis of the effects of parameter uncertainty in deterministic
623 hydrologic models. *Water Resour. Res.*, **12,** 925-932.

624 Xia, Y., and Coauthors, 2012: Continental-scale water and energy flux analysis and validation
625 for the North American Land Data Assimilation System project phase 2 (NLDAS-2): 1.
626 Intercomparison and application of model products. *J. Geophys. Res.: Atmos.*, **117,** D3.

Manuscript (Tables and Figures)
Click here to download Manuscript (my-two-LaTeX) Tables and Figures.docx

**Table 1 Nameid forty-two largest hurricane-season storms in North Carolina during year 1985 to 2012**

| No | Event name | Event Date | Event size (m) | Streamflow response size (m) | Antecedent soil moisture | Dominant control |
|---|---|---|---|---|---|---|
| 1 | Tropical storm Juan | 10/30/1985 | 0.108 | 0.033 | 0.21 | *d* |
| 2 (C) | Tropical storm Kate* | 11/20/1985 | 0.067 | 0.044 | 0.76 | *d* |
| 3 | Hurricane Charley | 8/16/1986 | 0.092 | 0.022 | 0.31 | *et* |
| 4 | Tropical depression Nine | 9/3/1987 | 0.098 | 0.027 | 0.03 | *d* |
| 5 | Tropical depression Chris* | 8/28/1988 | 0.067 | 0.008 | 0.01 | *d* |
| 6 | Tropical storm Isaac | 10/2/1988 | 0.061 | 0.007 | 0.11 | *d* |
| 7 | Tropical storm Barry | 7/15/1989 | 0.052 | 0.006 | 0.20 | *et* |
| 8 (B) | Hurricane Klaus | 10/10/1990 | 0.101 | 0.018 | 0.09 | *d* |
| 9 | Hurricane Lili | 10/22/1990 | 0.083 | 0.043 | 0.47 | *d* |
| 10 | Tropical storm Ana | 9/24/1991 | 0.076 | 0.015 | 0.17 | *d* |
| 11 | Tropical depression Two | 7/25/1994 | 0.064 | 0.001 | 0.22 | *et* |
| 12 | Hurricane Allison | 6/9/1995 | 0.052 | 0.015 | 0.46 | *et* |
| 13 (D) | Tropical Depression Jerry* | 8/25/1995 | 0.067 | 0.009 | 0.50 | *et* |
| 14 | Hurricane Opal | 10/3/1995 | 0.073 | 0.013 | 0.14 | *d* |
| 15 | Tropical storm Sebastien | 10/20/1995 | 0.054 | 0.018 | 0.30 | *d* |
| 16 | Hurricane Fran | 9/3/1996 | 0.063 | 0.001 | 0.09 | *d* |
| 17 | Hurricane Danny | 7/22/1997 | 0.060 | 0.004 | 0.11 | *d* |
| 18 | MH Erika | 9/9/1997 | 0.064 | 0.010 | 0.00 | *d* |
| 19 | Hurricane Earl* | 9/3/1998 | 0.068 | 0.006 | 0.05 | *d* |
| 20 | Hurricane Dennis | 8/25/1999 | 0.055 | 0.003 | 0.05 | *d* |
| 21 | Hurricane Dennis | 9/4/1999 | 0.149 | 0.071 | 0.17 | *d* |
| 22 | Hurricane Floyd | 9/14/1999 | 0.115 | 0.060 | 0.31 | *et* |
| 23 (A) | Tropical Storm Harvey | 9/27/1999 | 0.102 | 0.036 | 0.43 | *d* |
| 24 | Tropical Storm Gustav | 8/29/2002 | 0.074 | 0.014 | 0.35 | *et* |
| 25 | Tropical Storm Kyle | 10/10/2002 | 0.140 | 0.077 | 0.06 | *d* |
| 26 | Tropical Depression Bill | 7/1/2003 | 0.054 | 0.019 | 0.49 | *et* |
| 27 | Hurricane Isabel | 9/18/2003 | 0.055 | 0.010 | 0.21 | *d* |
| 28 | Hurricane Juan | 9/22/2003 | 0.053 | 0.023 | 0.55 | *et* |
| 29 | Tropical Storm Bonnie | 8/13/2004 | 0.062 | 0.007 | 0.38 | *et* |
| 30 | Tropical Depression Gaston | 8/29/2004 | 0.060 | 0.017 | 0.19 | *et* |
| 31 | Tropical Storm Alberto | 6/13/2006 | 0.051 | 0.016 | 0.41 | *et* |
| 32 | Tropical Storm Ernesto | 8/30/2006 | 0.073 | 0.006 | 0.01 | *d* |
| 33 | Hurricane Isaac | 10/5/2006 | 0.052 | 0.014 | 0.30 | *d* |
| 34 | Hurricane Noel | 10/24/2007 | 0.119 | 0.026 | 0.06 | *d* |
| 35 | MH Gustav | 8/25/2008 | 0.131 | 0.049 | 0.04 | *d* |
| 36 | Hurricane Hanna | 9/5/2008 | 0.109 | 0.075 | 0.25 | *et* |
| 37 | Tropical Depression One | 6/4/2009 | 0.072 | 0.015 | 0.15 | *et* |
| 38 | Hurricane Ida | 11/10/2009 | 0.139 | 0.058 | 0.35 | *d* |
| 39 | Hurricane Igor | 9/26/2010 | 0.151 | 0.048 | 0.02 | *d* |
| 40 | Hurricane Irene | 9/5/2011 | 0.061 | 0.010 | 0.01 | *d* |
| 41 | Tropical storm Debby | 7/9/2012 | 0.057 | 0.008 | 0.17 | *et* |
| 42 | Hurricane Sandy | 9/17/2012 | 0.061 | 0.004 | 0.08 | *d* |

- identifies events that have been highlighted in the shaded column in Fig. 1. *d* and *et* identify the dominant control on streamflow response to large hurricane season storms. *d* ≡soil moisture deficit; *et* ≡ evapotranspirative loss.

**Table 2 Key water balance statistics for calibration year**

| Precipitation (m) | Observed annual streamflow (m) | Simulated annual streamflow (m) | Total ET (m) | Observed Runoff Ratio | Modeled Runoff Ratio |
|---|---|---|---|---|---|
| 1.139 | 0.244 | 0.250 | 0.622 | 0.214 | 0.219 |

**Table 3 Water partitioning across different water stores for event pairs (A, B) and (C, D) (identified in Fig. 4)). (A1, A2 and A3) are ancillary event simulations with exactly the same forcings as event A, but with (all, only groundwater, only surface soil moisture) antecedent conditions being respectively identical to event B. (C1, C2 and C3) are same as event C but (happen at same time as event D, has antecedent conditions identical to event D, and have both antecedent condition and timing of event D), respectively.**

| | **Storm properties** | | **Antecedent conditions** | | **Water budget partition** | | | | **Changes in water budget partitions between event pairs** | | | |
|---|---|---|---|---|---|---|---|---|---|---|---|---|
| ***Event*** | ***Timing*** | ***P* (m)** | ***SS*** | ***GW* (m)** | ***eventQ* (m)** | ***eventQ/P*** | ***delS* (m)** | ***et* (m)** | Δ | **Δ*eventQ* *(m)*** | **-Δ*delS* (m)** | **-Δ*et* (m)** |
| A | Sept. | 0.102 | 0.43 | -9.2 | 0.036 | 0.35 | 0.054 | 0.012 | B-A | -0.018 | -0.015 | -0.002 |
| B | Oct. | 0.101 | 0.09 | -10.3 | 0.018 | 0.18 | 0.069 | 0.014 | | | | |
| A1 | Sept. | 0.102 | 0.09 | -10.3 | 0.02 | 0.2 | 0.072 | 0.01 | A1-A | -0.016 | -0.018 | 0.002 |
| A2 | Sept. | 0.102 | 0.43 | -10.3 | 0.034 | 0.33 | 0.057 | 0.011 | A2-A | -0.002 | -0.003 | 0.001 |
| A3 | Sept. | 0.102 | 0.09 | -9.2 | 0.021 | 0.21 | 0.07 | 0.011 | A3-A | -0.015 | -0.016 | 0.001 |
| C | Nov. | 0.067 | 0.76 | -6.5 | 0.044 | 0.66 | 0.016 | 0.007 | D-C | -0.035 | -0.011 | -0.024 |
| D | Aug. | 0.067 | 0.50 | -7.5 | 0.009 | 0.13 | 0.027 | 0.031 | | | | |
| C1 | Aug. | 0.067 | 0.76 | -6.5 | 0.031 | 0.46 | 0.001 | 0.035 | C1-C | -0.013 | 0.015 | -0.028 |
| C2 | Nov. | 0.067 | 0.50 | -7.5 | 0.023 | 0.34 | 0.038 | 0.006 | C2-C | -0.021 | -0.022 | 0.001 |
| C3 | Aug. | 0.067 | 0.50 | -7.5 | 0.007 | 0.10 | 0.026 | 0.034 | C3-C | -0.037 | -0.010 | -0.027 |

**Figure captions**

Figure 1 Observed stream flow responses (*eventQ)* due to large hurricane-season events (magnitude larger than 0.016m) ..... 34

Figure 2 (a) North Carolina county map, with LMW watershed location (shown in red dot), (b) Precipitation (July 2002), (c) Temperature (July 2002), (d) Elevation, (e) Land Cover and (f) Soil Map, of Lake Michie watershed ..... 35

Figure 3 Comparison of modeled and observed: (a) discharge during calibration period, (b) discharge during the entire simulation period (1985-2012), (c) groundwater heads at 36 locations in Lake Michie Watershed, and (d) Soil moisture deficit at the ECONET site (soil moisture deficit = 1 – soil saturation) ..... 36

Figure 4 Variation of (a) streamflow magnitude (*eventQ*), and (b) streamflow magnitude per unit event size (*eventQ/p*), with event precipitation size for the largest 50 storm events in the hurricane season in Lake Michie Watershed ..... 37

Figure 5 (a) Average soil saturation (SS) and groundwater table depth (GW) for events A and B, (b) Percentage of watershed area near saturation (Percent_SS) and area with groundwater table hitting the land surface (Percent_GW) for events A and B, (c) Soil saturation (SS) and overland flow depth (OVL) for event A (d) Soil saturation (SS) and overland flow depth (OVL) for event B ..... 38

Figure 6 Linear regression between (a) precipitation magnitude (*p*) and streamflow magnitude (*eventQ*), (b) effective precipitation (*effP=p-d*) and *eventQ*, (c) effective precipitation (*effP=p-et*) and *eventQ*, and (d) effective precipitation (*effP=p-et-d*) and *eventQ*. *d* is the moisture deficit in top 25 cms of soil, and *et* is the total evapotranspiration during an event ..... 39

Figure 7 Streamflow magnitude (*eventQ*) under different: antecedent soil moisture conditions in top soil layer (25 cm), timing of event, and storm size. $SM_d$, $SM_i$ *and* $SM_w$ indicate dry, intermediate and wet top soil saturation conditions, respectively; J, S and N indicate July, September and November, respectively; $P_i$, $P_l$ *and* $P_h$ indicate intermediate, low and high precipitation magnitudes. ..... 40

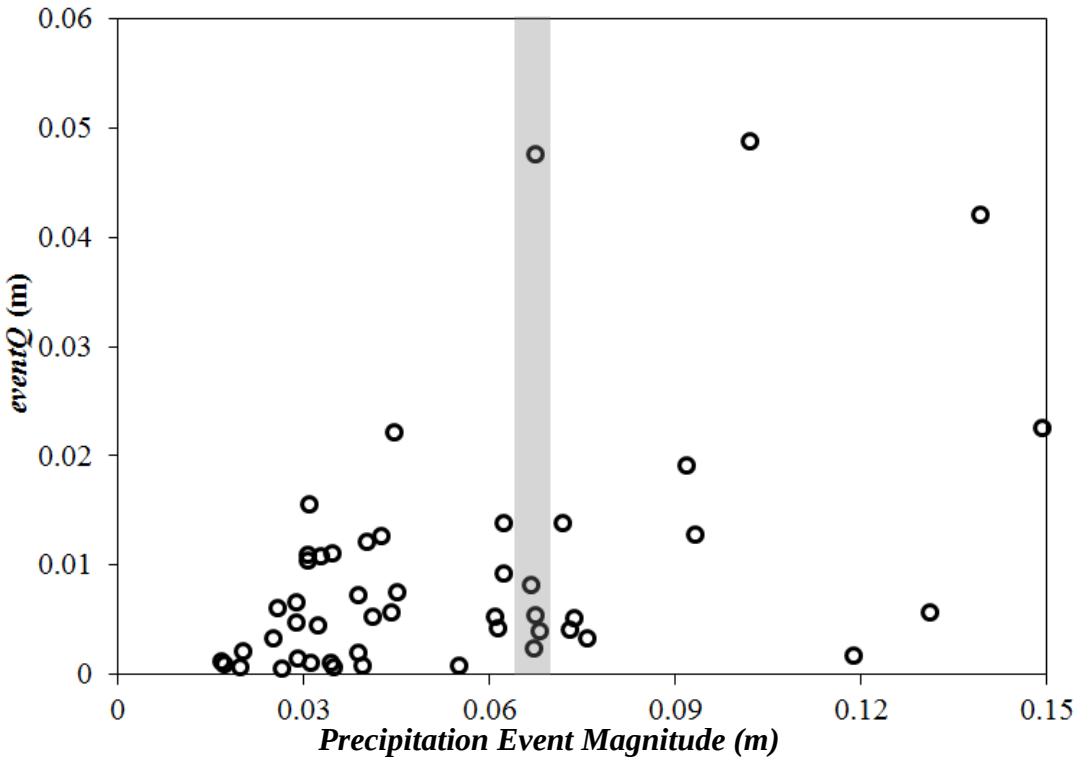


**Figure 1 Observed stream flow responses (*eventQ)* due to large hurricane-season events (magnitude larger than 0.016m)**

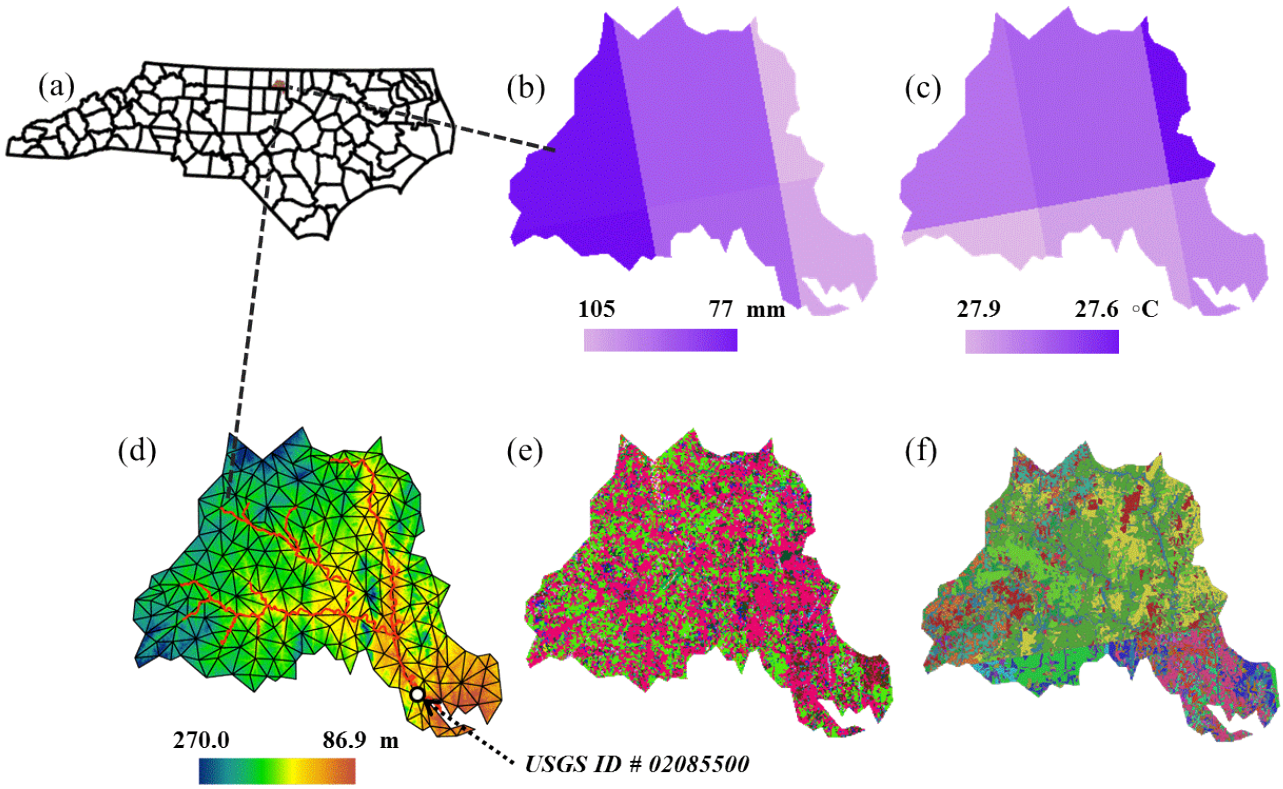


**Figure 2 (a) North Carolina county map, with LMW watershed location (shown in red dot), (b) Precipitation (July 2002), (c) Temperature (July 2002), (d) Elevation, (e) Land Cover and (f) Soil Map, of Lake Michie watershed**

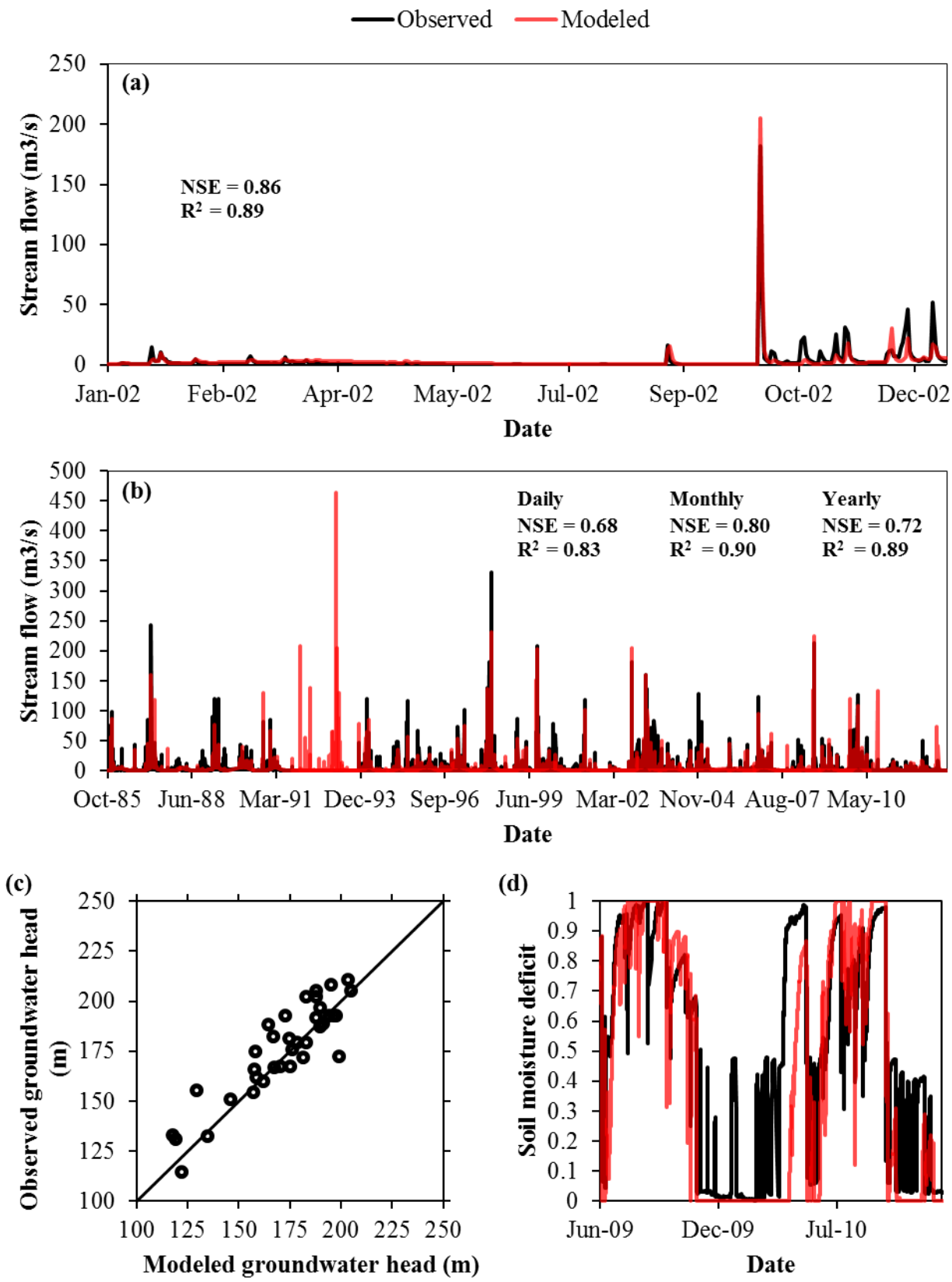


**Figure 3 Comparison of modeled and observed: (a) discharge during calibration period, (b) discharge during the entire simulation period (1985-2012), (c) groundwater heads at 36 locations in Lake Michie Watershed, and (d) Soil moisture deficit at the ECONET site (soil moisture deficit = 1 – soil saturation)**

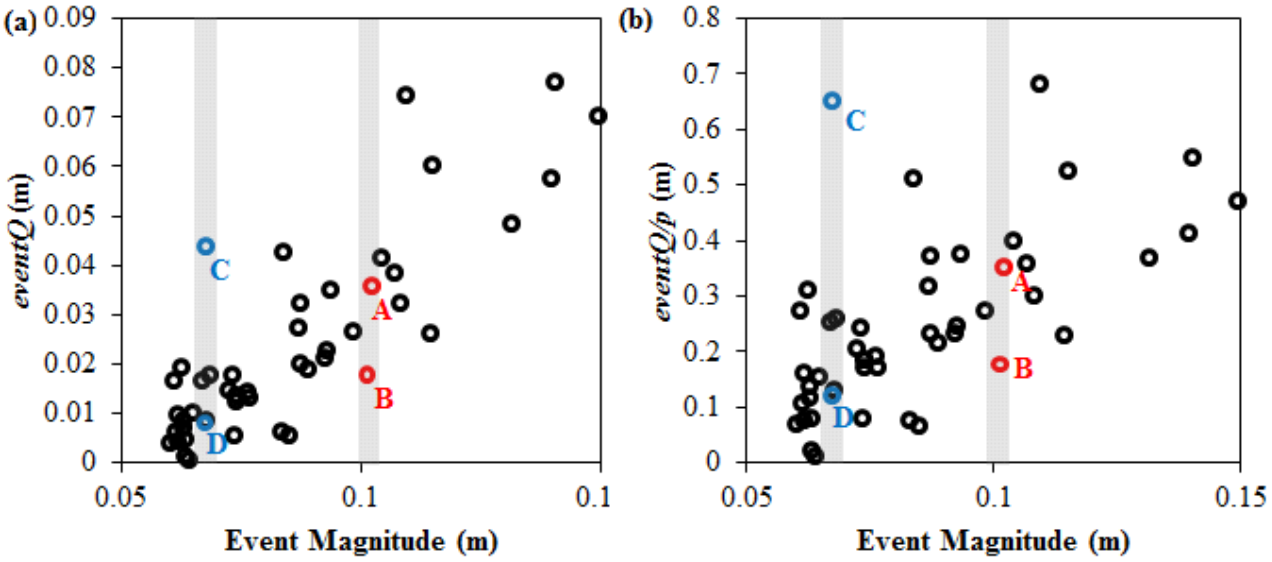


**Figure 4 Variation of (a) streamflow magnitude (*eventQ*), and (b) streamflow magnitude per unit event size (*eventQ/p*), with event precipitation size for the largest 50 storm events in the hurricane season in Lake Michie Watershed**

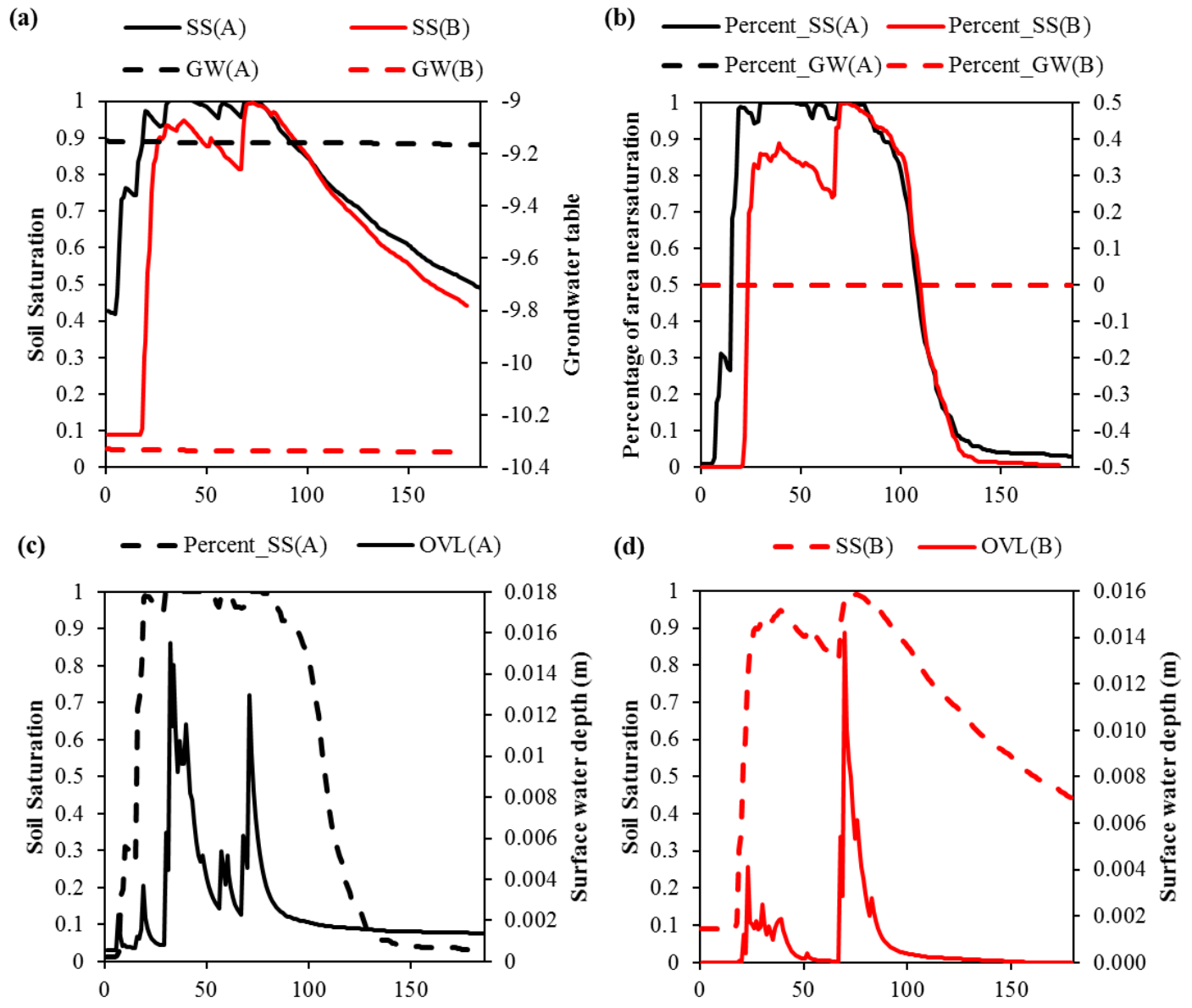


**Figure 5 (a) Average soil saturation (SS) and groundwater table depth (GW) for events A and B, (b) Percentage of watershed area near saturation (Percent_SS) and area with groundwater table hitting the land surface (Percent_GW) for events A and B, (c) Soil saturation (SS) and overland flow depth (OVL) for event A (d) Soil saturation (SS) and overland flow depth (OVL) for event B**

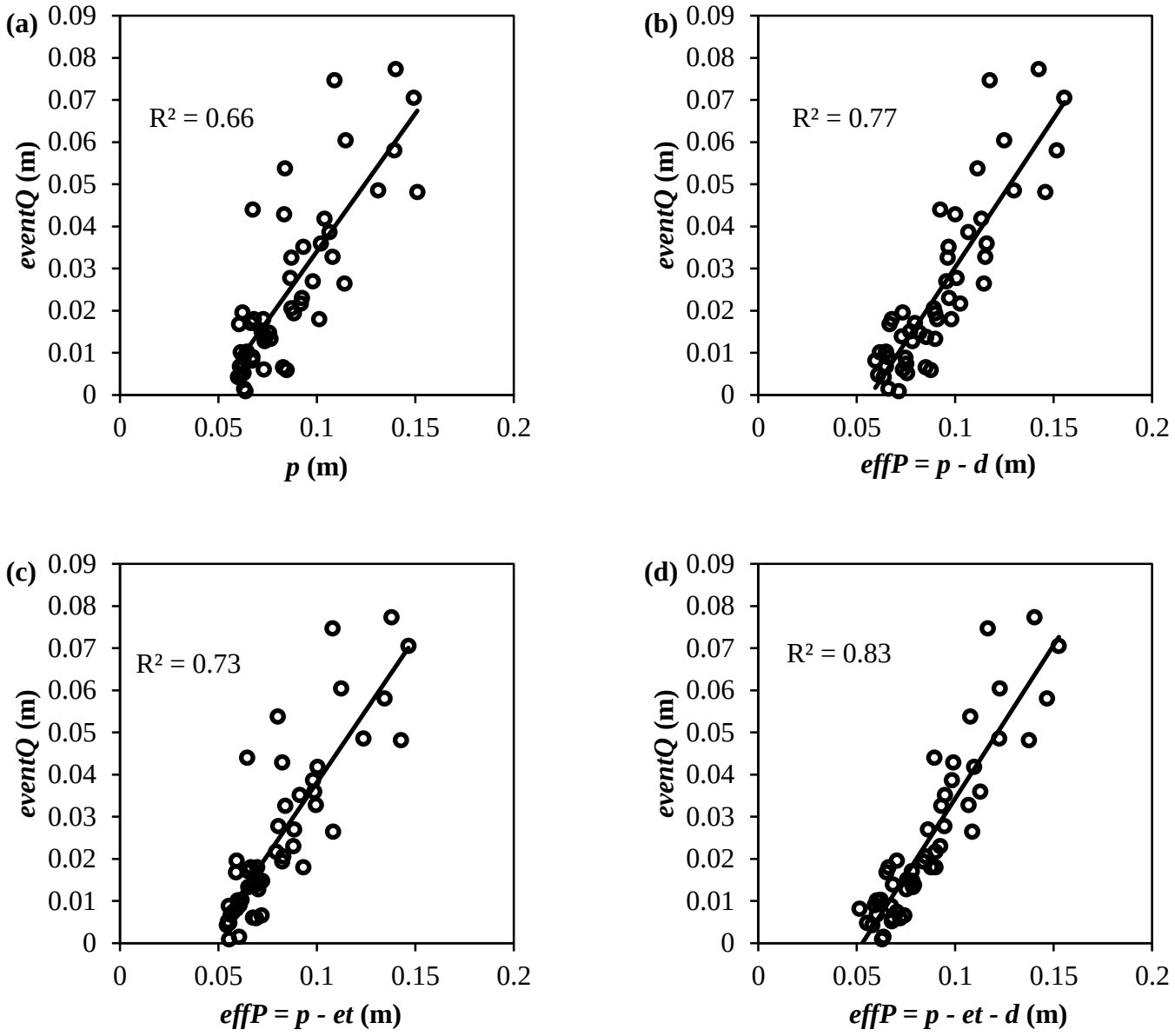


**Figure 6 Linear regression between (a) precipitation magnitude (*p*) and streamflow magnitude (*eventQ*), (b) effective precipitation (*effP=p-d*) and *eventQ*, (c) effective precipitation (*effP=p-et*) and *eventQ*, and (d) effective precipitation (*effP=p-et-d*) and *eventQ*. *d* is the moisture deficit in top 25 cms of soil, and *et* is the total evapotranspiration during an event**

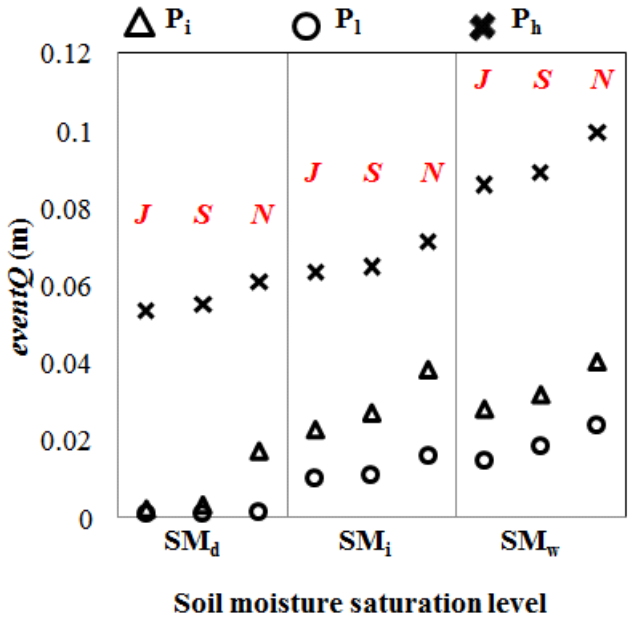


**Figure 7 Streamflow magnitude (*eventQ*) under different: antecedent soil moisture conditions in top soil layer (25 cm), timing of event, and storm size. $SM_d$, $SM_i$ and $SM_w$ indicate dry, intermediate and wet top soil saturation conditions, respectively; J, S and N indicate July, September and November, respectively; $P_i$, $P_l$ and $P_h$ indicate intermediate, low and high precipitation magnitudes.**